

## The X-ray emission of the Crab-like pulsar PSR J0537–6910

T. Mineo<sup>a</sup>, G. Cusumano<sup>a</sup> and E. Massaro<sup>b</sup>

<sup>a</sup>Istituto di Astrofisica Spaziale e Fisica Cosmica, CNR, Sezione di Palermo, via U. La Malfa 173, I-90139, Palermo, Italy

<sup>b</sup>Dipartimento di Fisica, Università la Sapienza, Piazzale A. Moro 2, I-00185, Roma, Italy

In this paper we present some preliminary result on the spectral and timing analysis of the X-ray pulsed emission from the 16 ms pulsar PSR J0537–6910 in the energy range 0.1–30 keV, based on archival BeppoSAX and RossiXTE observations. This pulsar, discovered by Marshall et al. [1] in the LMC field with RXTE, is the fastest spinning pulsar associated with a supernova remnant. It is characterized by strong glitch activity with the highest rate of all known Crab-like system.

### 1. INTRODUCTION

PSR J0537–6910 is a Crab-like pulsar embedded in the supernova remnant N157B in the 30 Doradus region located near the centre of the LMC. This supernova belongs to the rare class of Crab-like remnants [2] distinguished by their centrally-filled morphology and non-thermal X-ray spectra, whose emission is predominantly powered by the young pulsar at the center. PSR J0537–6910 is the most rapidly rotating pulsar associated with a SNR ( $P=16.1$  ms), twice as fast as the Crab pulsar, with a period derivative of  $\dot{P}=5.17 \times 10^{-14}$  s s<sup>-1</sup>, a rotational energy loss rate of  $\dot{E} = 4.8 \times 10^{38}$  erg s<sup>-1</sup>, a magnetic field at the neutron star surface of  $B_s = 9.2 \times 10^{11}$  G and a braking age of  $\tau = 5.0 \times 10^3$  yr in agreement with the predicted SNR age [3]. It represents the oldest known Crab-like pulsar.

Pulsed emission was first discovered in the X-ray range by RXTE/PCA [1] and soon after confirmed by BeppoSAX [4] and ROSAT/HRI [5]. The light curve is characterized by a narrow pulse shape with a full width duty cycle of about 10% [6,5]. The 2–10 keV pulsed spectrum has been modeled with a simple power law: RXTE+ASCA measured a spectral index of  $1.6 \pm 0.4$  and a 2–10 flux of  $(6.7 \pm 0.6) \times 10^{-13}$  erg cm<sup>-2</sup> s<sup>-1</sup> [1], in agreement with the BeppoSAX values of  $1.1 \pm 0.4$  and  $(5.1 \pm 1.1) \times 10^{-13}$  erg cm<sup>-2</sup> s<sup>-1</sup> [4].

The source shows intense glitch activity: 6 glitch events, with a mean amplitude in the frequency change of  $\Delta\nu/\nu=0.36 \times 10^{-6}$ , have been observed during the almost 3 years monitoring campaign performed by RXTE [7]. No pulsed emission has been detected at radio wavelengths thus far [6].

### 2. OBSERVATION AND DATA REDUCTION

The RXTE observations considered in our analysis were performed between 26 March and 19 December 2001. We used the PCA [8] data accumulated in "Good Xenon" telemetry mode (1 $\mu$ s accuracy) selecting all detector layer to increase the S/N ratio of the pulsation. Standard selection criteria were applied on the observation data excluding time intervals corresponding to South Atlantic Anomaly passages and when the Earth limb was less than 10° from the pointing and when the angular distance between the source position and the pointing of the satellite was larger than 0.02°. All analysed observations were pointed at PSR J0537–6910 and relate to the same gain epoch. The total exposure time is about 1300 ks.

The narrow field instruments onboard BeppoSAX [9] observed the LMC field several times during its life. For our analysis, we selected the observations pointed at N157B and considered data from the two imaging detectors LECS (0.1–

10 keV) and MECS (1.6–10 keV) for a total exposure of 29 ks and 89 ks, respectively. In both instruments, events were extracted from a circular region centred at the source position with a radius of 3' which maximizes the signal-to-noise ratio of the pulsed component. The LBCS energy range 0.1–1.0 keV was not included in the analysis because of the low statistical significance of the pulsed emission due to a contribution from the hot gas of 30 Doradus [4].

### 3. TIMING ANALYSIS

The UTC arrival times of all selected events were first converted to the Solar System Barycentre using the (J2000) pulsar position  $\alpha = 5^h 37^m 47.2^s$  and  $\delta = -69^\circ 10' 23''$  [5] and the JPL2000 planetary ephemeris (DE200, [10]). For each observation, we searched the pulsed frequency  $\nu$  using the folding technique in a range centred at the value computed with the pulsar ephemeris reported by [7]. The central time of each observation was chosen as reference epoch and the corresponding frequency was estimated by fitting the  $\chi^2$  peak with a gaussian. Frequency errors at  $1\sigma$  level were computed from the interval corresponding to a unit decrement with respect to the maximum in the  $\chi^2$  curve. The top panel of Fig. 1 shows the frequencies obtained for BeppoSAX (triangles) and RXTE (stars) together with the linear ephemeris quoted by [7] (dashed line); residuals with respect to this relation are presented in the bottom panel. Note that they are positive around the value of  $2 \times 10^{-5}$  Hz until MJD 52157, and afterwards show a rather regular decrease to negative values over a time span of about 100 days, indicating the occurrence of timing activity in this young pulsar.

The highest significance of the pulsation is reached in the energy intervals 2.5–30 keV in RXTE data and 1.0–10 keV in BeppoSAX data. The RXTE profile is shown in Fig. 2: it is characterized by a narrow single peak with a duty cycle of 0.28 at zero level. Fitting the peak with a gaussian, a value of  $0.11 \pm 0.07$  is obtained for the FWHM, compatible with the value obtained with ROSAT [5] and Chandra data [6].

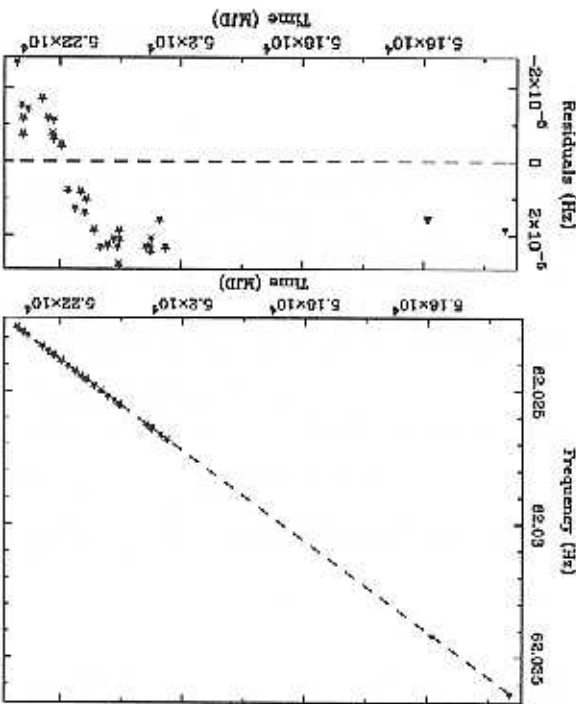


Figure 1. PSR J0537–6910 frequency evolution (top panel) and residuals (bottom panel) with respect to the [7] relation (dashed line). BeppoSAX data are indicated with triangles; RXTE data with stars.

### 4. SPECTRAL ANALYSIS

Pulse phase histograms were accumulated for each unit and for each observation of the PCA independently for the 256 PHA channels. The same procedure has been applied to MECS data. RXTE response matrices were derived for each unit and summed together weighting with the background subtracted counts of the correspondent PCU's phase histograms. RXTE spectra were combined by summing the individuals units and assigning a total exposure time equal to the sum of the individual exposures. The spectral distribution of the pulsed signal was accumulated in the phase interval 0.64–0.84 subtracting the off-pulse level evaluated in the phase range 0.0–0.5. The two phase regions considered in our analysis

Table 1  
Best fit parameters

	Simple power law	Curved power law
$N_H$ ( $\text{cm}^{-2}$ )	$(1.3 \pm 0.5) \times 10^{22}$	$(1.4 \pm 0.7) \times 10^{22}$
$\alpha$	$1.67 \pm 0.07$	$1.33 \pm 0.12$
$\beta$	–	$0.15 \pm 0.05$
$\chi^2$ (dof)	67.2 (82)	60.2 (81)

are indicated in Fig. 2.

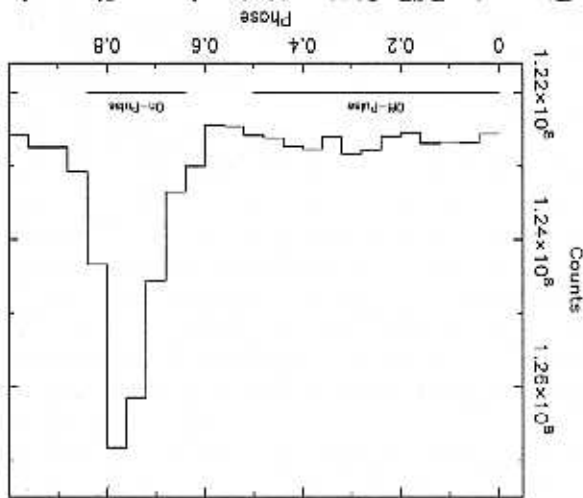
The *BeppoSAX* and *RXTE* spectra covering the energy range 1.0–30 keV were fitted together. The inter-calibration factors were fixed to the values derived fitting the common energy interval 2–10 keV; in particular the value  $0.9 \pm 0.3$  has been derived for *IECS-MECS* and  $1.19 \pm 0.09$  for *XTE-MECS*. The spectra have been modeled with a simple power law whose best fit parameters are shown in Table 1. The best fit parameters of the simple power law are in agreement with the previous evaluations [4,5] and, according to the  $\chi^2$  value, this model well represents the spectrum over the whole range. The detected 2–10 unabsorbed flux is  $(7.3 \pm 0.5) \times 10^{-13}$  erg  $\text{cm}^{-2}$   $\text{s}^{-1}$ , corresponding to a luminosity of  $1.9 \times 10^{35}$  erg  $\text{s}^{-1}$  for an estimated distance of 47 kpc [11]. Table 1 shows the best fit result. A second model has been investigated: a curved power law characterized by a linear dependence of the spectral slope upon the logarithm of energy:

$$F(E) = K E^{-(\alpha + \beta \log(E))} \quad (1)$$

We presented some preliminary results on the spectral and timing analysis of the X-ray pulsed emission of the 16 ms pulsar PSR J0537–6910 in the energy range 1.0–30 keV, based on archival *BeppoSAX* and *RossixXTE* observations. The detected profile is characterized by a narrow single peak with a duty cycle of 0.28 at zero level. The pulsed spectrum has been fitted with two models: the simple power law and a curved power law. The simple power law gave acceptable  $\chi^2$ , but the introduction of the curvature parameter  $\beta$  is significant at 99.7% confidence level. This result suggests that the photon index softens at

## 5. CONCLUSION

Figure 2. PSR J0537–6910 pulse profile in the energy range 2.5–30 keV obtained with *RXTE* data. The on-source and background phase intervals used for the spectral analysis are also indicated.





higher energies. The value of the bending parameters is compatible within the errors with the values and for the other Crab-like pulsars Crab [12], PSR B1509-58 [13], PSR B0540-69 [14]. According to the measured parameters of the curved model, the SED of the pulsed emission has a maximum at energy

$$E_m = 10^{(2-\alpha)/(2\beta)} \quad (2)$$

which correspond to  $\sim 170$  keV, practically coincident with the value measured for the interpulse of the Crab pulsar [13].

The models that have been proposed to explain high energy emission from pulsars can be classified in two distinct classes, outer gap [15] and polar gap models [16], depending on the location of the emitting region. In the framework of the outer gap model, the energy of the maximum follows the appropriate scaling relation with respect to the interpulse emission of the Crab as observed for the PSR B1509-58 [13].

REFERENCES

1. Marshall et al., *Apl* 499 (1998) L179.
2. F.D. Seward, *SSR* 49 (1989) 385.
3. Q.D. Wang and E.V. Gotthelf, *Apl* 494 (1998) 623.
4. G. Cusumano, et al., *A&A* 335 (1998) L55.
5. Q.D. Wang and E.V. Gotthelf, *Apl* 509 109 (1998).
6. Q.D. Wang, et al., *Apl* 559 (2001) 275.
7. E.V. Gotthelf, et al., *Neutron Stars in Supernova Remnants*, ASP Conference Series, Vol. 9999, P.O. Stone and B.M. Gaensler, eds. (2002).
8. K. Jahoda, et al., *SPE*, 2808, 59 (1996).
9. G. Boella et al., *A&AS* 122 (1997) 299.
10. E.M. Standish, *A&A* 114 (1982) 297.
11. A. Gould, *Apl* 452 (1995) 189.
12. E. Massaro, et al., *A&A* 361 (2000) 695.
13. G. Cusumano, et al., *A&A* 375 (2001) 404.
14. T. de Pla, et al., *A&A*, 499, 1013 (2003).
15. K. Cheng, et al., *Apl* 300 (1986) 522.
16. J.K. Daugherty and A.K. Harding, *Apl* 429 (1994) 325.